

A Multi-Heme Flavoenzyme as a Solar Conversion Catalyst

Andreas Bachmeier, Bonnie J. Murphy, and Fraser A. Armstrong*

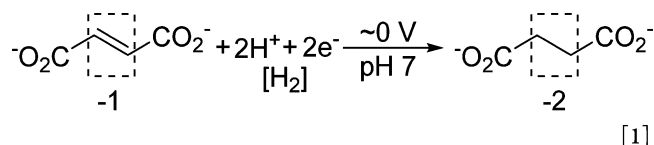
Inorganic Chemistry Laboratory, Department of Chemistry, University of Oxford, South Parks Road, Oxford OX1 3QR, United Kingdom

S Supporting Information

ABSTRACT: The enzyme flavocytochrome c_3 (fcc_3), which catalyzes hydrogenation across a C=C double bond (fumarate to succinate), is used to carry out the fuel-forming reaction in an artificial photosynthesis system. When immobilized on dye-sensitized TiO_2 nanoparticles, fcc_3 catalyzes visible-light-driven succinate production in aqueous suspension. Solar-to-chemical conversion using neutral water as the oxidant is achieved with a photoelectrochemical cell comprising an fcc_3 -modified indium tin oxide cathode linked to a cobalt phosphate-modified $BiVO_4$ photoanode. The results reinforce new directions in the area of artificial photosynthesis, in particular for solar-energy-driven synthesis of organic chemicals and commodities, moving away from simple fuels as target molecules.

Artificial photosynthesis (AP) seeks to convert sunlight to storable chemical energy, i.e., fuels. “Solar fuels” have the potential both to address the world’s growing energy demand and to reduce greenhouse gas emissions caused by combustion of fossil fuels.¹ Building on the principles of natural photosynthesis, light harvesting and charge separation are coupled by electron transfers (ETs) to fuel formation and O_2 evolution at efficient and specific catalysts. For commercial viability, an AP system must not only be intrinsically simpler in design than the complex photosynthetic enzymes but should also be efficient and stable and comprise earth-abundant, inexpensive materials. Despite major research efforts and significant progress,^{2–5} the search for “champions” is slow, and major scientific breakthroughs are needed to fulfill all the above-mentioned criteria. Currently, AP research is focused on H_2 production or reduction of CO_2 , but the low-value products have little immediate opportunity to compete with fossil fuels. One way to bridge the gap is to identify reactions that could be driven by an AP system, especially the synthesis of high-value organic chemicals.^{6–10} Such a diversion from conventional paths is intellectually desirable and could attract more immediate commercial interest.

This paper concerns initial experiments to expand the repertoire of fuel-forming reactions to include reductions of organic molecules, and we herein present an enzyme-based photocatalytic system that helps to level the above-mentioned hurdles at the bench scale. Catalytic reduction of fumarate to succinate (eq 1) is equivalent to hydrogenation across a C=C bond (with each olefinic carbon changing oxidation number from -1 to -2). Used in an AP system, it exemplifies direct conversion of hydrogen into storable organic molecules, not unlike photosynthetic hydrogen fixation as NADPH.¹¹



This reaction is catalyzed by flavocytochrome c_3 (fcc_3) from *Shewanella frigidimarina* NCIMB400 (Figure 1). Although succinate itself is not a high-value chemical, a demonstration of its “photosynthesis” may stimulate new directions and possibilities for enzymes in the light-driven transformation of organic chemicals. Enzymes are highly selective catalysts that are already used in the chemical industry; vast libraries are available, and the development of suitable examples for AP may further increase their commercial usage.

Figure 1 depicts fcc_3 adsorbed on a TiO_2 surface. The enzyme has four heme groups that collect and relay electrons to the flavin (FAD) active site. A further important feature of fcc_3 is that both FAD and heme centers strongly absorb visible light:¹³ the kinetics of the entire ET process, from the excited light absorber to catalytic conversion at the active site, are thus amenable to time-resolved optical techniques.

To establish whether fcc_3 can be incorporated into an AP system, we first studied its electroactivity when it is immobilized on electrodes and light-harvesting components. We explored the interaction of fcc_3 with different electrodes using protein film

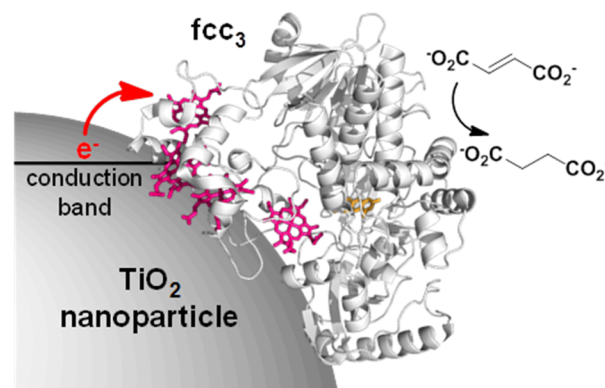


Figure 1. Cartoon showing flavocytochrome c_3 (PDB structure 1QJD¹²) adsorbed on a TiO_2 surface. Intramolecular ET to and from the flavin active site occurs over a distance of up to ca. 40 Å via four visible-light-absorbing heme groups (pink) that are close to the enzyme surface.

Received: July 29, 2014

Published: September 9, 2014

electrochemistry (PFE), a suite of techniques revealing intricate mechanistic details of redox enzymes under turnover conditions.¹⁴ Experimental details are given in the Supporting Information (SI). Figure 2 compares the electrocatalytic reduction of fumarate by fcc_3 adsorbed on the n-type semiconductor electrodes TiO_2 and CdS with results obtained using “pyrolytic graphite edge” (PGE) and mesoporous indium tin oxide [meso-ITO, 10% Sn(IV)-doped In_2O_3].^{15,16} Cyclic voltammograms (CVs) recorded on a rotating-disc PGE and a stationary ITO electrode are shown in Figure 2A,B, where the peaklike Faradaic current observed for the latter is due to substrate depletion, as expected under the stationary conditions. The two reduction waves display similar onset potentials (ca. -0.05 V vs SHE at pH 7), reflecting the fact that this parameter is controlled by the redox properties of the enzyme, provided that the electrode behaves like a metal.^{17–19} The results for PGE agree well with previous reports.²⁰

The electrocatalytic behavior of fcc_3 on TiO_2 and CdS electrodes is shown in Figure 2C,D. In contrast to PGE and ITO, the onset of the catalytic current commences at much higher overpotentials on both semiconductor materials. The negative shift in onset potential reflects the limited surface electron availability at the semiconductor–catalyst interface when the applied potential is well away from the semiconductor flatband potential (E_{fb}). For an n-type semiconductor, the majority carrier (i.e., electron) availability increases exponentially as E_{fb} is approached.²¹ Figure S1 in the SI makes this feature even more prominent by directly comparing the background-subtracted CVs obtained on all four electrodes.

The catalytic onset potentials for fumarate reduction on TiO_2 and CdS are similar, which can be ascribed, at least in part, to their relatively similar E_{fb} .¹⁷ Our observations reaffirm that carrier availability and E_{fb} have a profound impact on electrocatalytic activity, an effect we have observed in previous experiments with hydrogenase and carbon monoxide dehydrogenase enzymes adsorbed on TiO_2 and CdS .¹⁷

Having established the electroactivity of fcc_3 on the semiconducting electrode materials CdS and TiO_2 , we assembled a photocatalytic system to check for visible-light-driven fumarate reduction based on dye-sensitized TiO_2 nanoparticles (NPs). The enzyme shows good stability when adsorbed on TiO_2 electrodes (CVs recorded 24 h after enzyme adsorption are shown in Figure S2). The TiO_2 NPs (anatase, 15 nm) were modified with fcc_3 and then sensitized with the visible-light-absorbing chromophore $[\text{Ru}^{\text{II}}(\text{bpy})_2(4,4'-(\text{PO}_3\text{H}_2)_2\text{bpy})]\text{Br}_2$ (RuP) (bpy = 2,2'-bipyridine) as used in previous studies^{22,23} to assemble the complete photocatalytic system. Uptake of both RuP and enzyme onto the TiO_2 NPs was quantified by analyzing the supernatant by UV/vis spectroscopy after centrifugation. Quantitative adsorption was obtained for 56 nmol of RuP and 1.95 nmol of fcc_3 on 5 mg of TiO_2 , corresponding to a surface coverage of up to 86% fcc_3 (depending on enzyme orientation; see the SI) and 25% RuP. Figure 3A shows a photograph of TiO_2 NPs modified with fcc_3 ; the pink color of the enzyme is clearly observable. The UV/vis spectra of an fcc_3 solution taken before and after adsorption on TiO_2 are presented in Figure 3B. No features due to fcc_3 are observed after 20 min of stirring with TiO_2 , confirming quantitative uptake. Details are given in the SI.

Photochemical fumarate reduction was carried out as follows: 1.95 nmol of fcc_3 and 56 nmol of RuP were coadsorbed on 5 mg of TiO_2 , which was suspended in 5 mL of deuterated 0.2 M 2-(*N*-morpholino)ethanesulfonic acid (MES) buffer containing 6 mM disodium fumarate. The MES also acts as a sacrificial electron

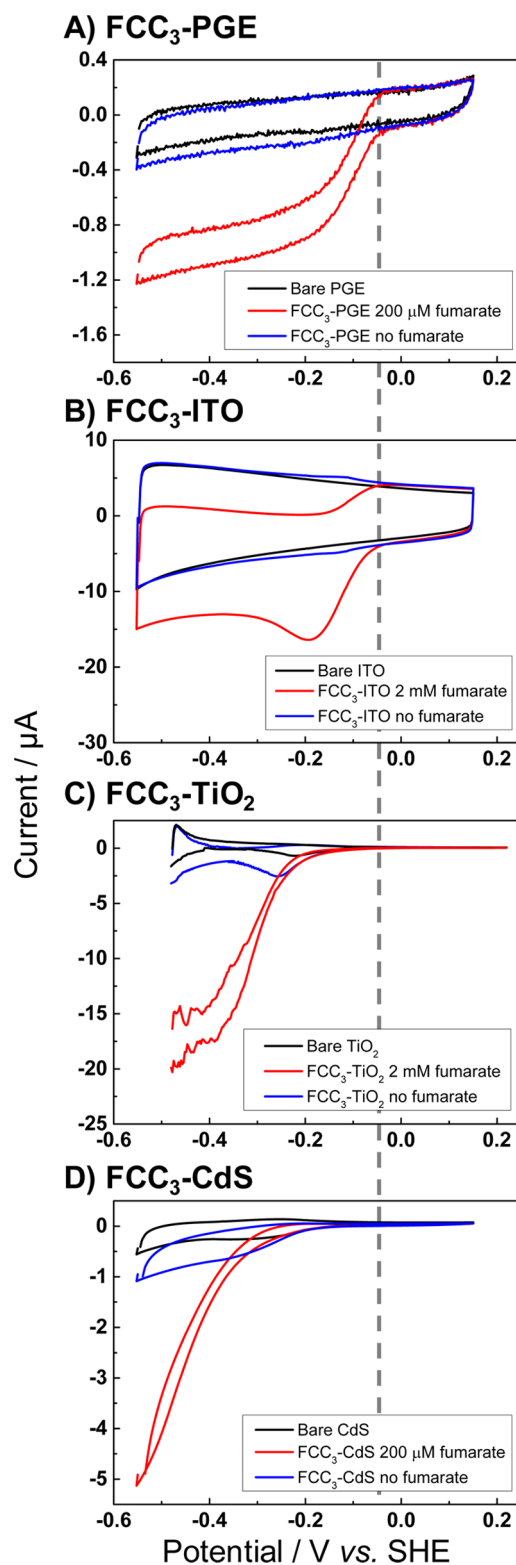


Figure 2. Cyclic voltammograms (20 mV s^{-1}) of unmodified (black, recorded in the presence of fumarate) and fcc_3 -modified electrodes (red, blue) in a mixed buffer system (pH 7.0) at 5°C in the presence of fumarate (red) and after removal of the substrate (blue), recorded (A) under rotation ($\omega = 2500 \text{ s}^{-1}$) and (B–D) with a stationary electrode with (A,B) no gas flow and (C,D) sparging of the solution with argon close to the working electrode. The dashed gray lines indicate the onset potential for fumarate reduction on PGE and ITO.

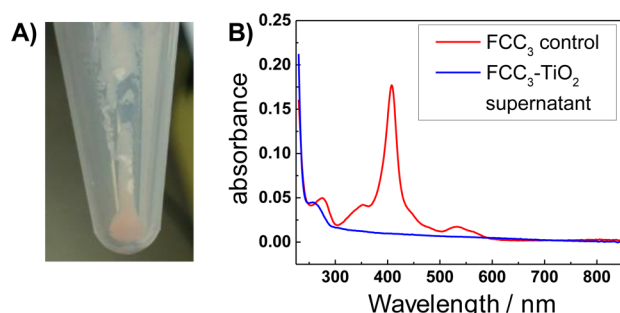


Figure 3. (A) Photograph of fcc_3 -modified TiO_2 NPs after centrifugation. The pink color is due to adsorbed fcc_3 . (B) Absorption spectra recorded before and after modification of TiO_2 with fcc_3 show quantitative adsorption.

donor. The stirred suspension was irradiated by a tungsten halogen lamp fitted with a 420 nm UV filter (45 mW cm^{-2} light intensity). Catalytic turnover was monitored by ^1H NMR spectroscopy. Spectra recorded after visible-light illumination of TiO_2 NPs modified with RuP and fcc_3 are shown in Figure S3 (NMR spectra were recorded after centrifugation of the reaction mixture). Succinate formation was confirmed by the ^1H NMR signal at 2.33 ppm, which increased when more succinate was added (Figure S3B inset). The succinate/fumarate ratio calculated after 4 h of irradiation (Figure S3A) corresponds to a turnover number (TON) of 5800 and an average turnover frequency (TOF) of 0.4 s^{-1} . Illumination over 8 h (Figure S3B) gave no significant enhancement in fumarate reduction, indicating that the maximum TON had already been reached after ca. 4 h. The average TOF of 0.4 s^{-1} is therefore a lower limit for what must be achievable under these reaction conditions. Under turnover conditions, the reaction mixture changed color from colorless to orange, indicating dissociation of the non-covalently bound flavin and/or the heme moieties (Figures S4 and S5). This instability is discussed below.

Mechanistically, visible-light excitation of RuP (giving RuP^*) injects electrons into the TiO_2 conduction band (CB); the electrons can then be transferred to fcc_3 . This “through-particle” pathway²⁴ was established by the following experiments. No succinate was formed after illumination for 4 h in the absence of TiO_2 (i.e., RuP and fcc_3 codissolved in MES/fumarate buffer; Figure S3C). A bimolecular reaction pathway between RuP^* and fcc_3 in solution is thus ruled out. Illumination of RuP and fcc_3 coadsorbed on ZrO_2 NPs instead of TiO_2 also yielded no detectable amounts of succinate after 4 h (Figure S3D). The CB energy of ZrO_2 is too negative to accept electrons from RuP^* .²⁴ Instead, this experimental configuration would only allow direct ET from surface-bound RuP^* to coadsorbed fcc_3 , which evidently does not occur. The reaction mixtures remained colorless in both types of “control” experiments, and the sensitized ZrO_2 particles retained their pink color after illumination, indicating that fcc_3 remained undamaged (Figures S4–S6). Taken together, these observations strongly suggest that enzyme degradation occurs only under photochemical turnover. A possible degradation route involves the powerfully oxidizing species RuP^+ , formation of which requires TiO_2 (RuP^+ is not formed when RuP is adsorbed on ZrO_2).

A full photosynthetic cycle using water as the electron donor was achieved using a photoelectrochemical cell in which a visible-light-responsive n-type W-BiVO_4 photoanode²⁵ was used as the counter electrode (CE) in a two-electrode configuration (Figure 4A). The CB potential of BiVO_4 (-0.39 V vs SHE at pH 7)²⁶

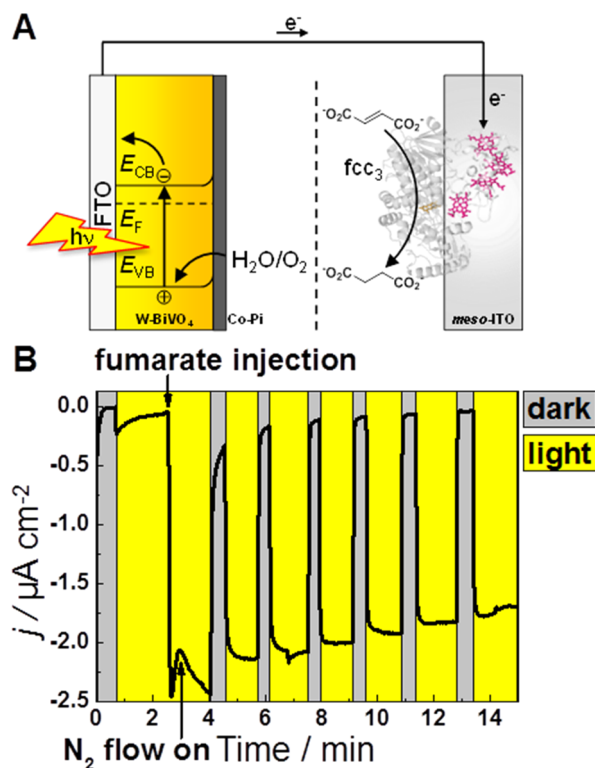


Figure 4. (A) Schematic of a photoelectrochemical cell comprising an fcc_3 -modified meso-ITO cathode (WE) and a Co-Pi-modified W-BiVO_4 photoanode (CE). (B) Photocurrent profile for visible-light-driven fumarate reduction. The cell solution was 0.1 M potassium phosphate (pH 7.0) at 25°C . The WE compartment was sparged with N_2 , but the gas flow was briefly stopped during injection of fumarate (to 2 mM) at $t = 2.5 \text{ min}$.

provides sufficient driving force to reduce fumarate at neutral pH without an externally applied bias. To enhance the water oxidation rate, the electrode was coated with a cobalt phosphate (Co-Pi) surface electrocatalyst²⁷ via photoassisted electro-deposition²⁸ (Figure S7). In a separate cell compartment (separated by a porous frit), a meso-ITO electrode modified with fcc_3 was used as the working electrode (WE).²⁹ The photoanode was irradiated through the FTO support (back illumination).³⁰

Figure 4B shows the photocurrent profile for the integrated system at neutral pH under zero external bias. In the absence of fumarate ($\Delta t = 0.7\text{--}2.5 \text{ min}$), only a small, rapidly decaying photocurrent is observed (note that the assembly does not provide enough driving force for H^+ reduction), similar to the bare ITO electrode (Figure S8). Injection of fumarate into the WE compartment at $t = 2.5 \text{ min}$ (final concentration 2 mM) causes an immediate step increase in the photocurrent as the charge-transport pathway becomes available and fumarate reduction takes place. Voltammograms of each electrode were recorded after the experiment to verify the activities of the components (Figure S9).

The overall “solar-to-succinate” efficiency (η_{sts}) can be determined according to eq 2, which is based on the expression³¹ that describes the efficiency of H_2O photoelectrolysis:

$$\eta_{\text{sts}} = j_{\text{ph}} \eta_f (0.79 \text{ V}) P_{\text{in}}^{-1} \quad (2)$$

where j_{ph} is the photocurrent density, η_f is the faradaic efficiency for fumarate reduction, 0.79 V is the potential that is theoretically

required to achieve both fumarate reduction and water oxidation (at pH 7, the fumarate/succinate potential is +0.03 V vs SHE,²⁰ and the H₂O/O₂ potential is +0.82 V vs SHE), and $P_{in} = 45 \text{ mW cm}^{-2}$ the incident light intensity. With $\eta_f = 100\%$ for fcc₃-catalyzed fumarate reduction as the upper limit (no significant photocurrent could be observed before the introduction of fumarate), $\eta_{sts} = 0.03\%$ at $t = 15 \text{ min}$. The estimated TOF per enzyme molecule is 0.01 s^{-1} , which is 1 order of magnitude lower than we obtained in photocatalytic conversion with RuP–TiO₂, where a sacrificial electron donor was used to drive the reaction (see SI). Efficiency limitations in these initial proof-of-principle experiments include irradiation with only the visible spectral region and detachment of the Co–Pi catalyst from the W–BiVO₄ surface (Figure S9), similar to observations made by Sivula and co-workers.³² Despite the low overall efficiency, the proof of principle is established, and there is large scope for improvement.

In conclusion, we have described the use of an enzyme that catalyzes C=C bond hydrogenation in two types of artificial photosynthetic systems, the implication being that AP with water oxidation can be extended to other enzymes/catalysts performing reductive transformations having greater value than bulk fuel formation. A further important factor is that enzymes like fcc₃ possessing intense chromophores may be exploited to elucidate ET kinetics by time-resolved spectroscopy. These results help highlight new directions for AP away from the traditional solar-to-fuels paradigm to more advanced solar-to-chemical conversions, also using water as the electron source.

■ ASSOCIATED CONTENT

■ Supporting Information

Full materials and methods; supplementary figures, including fcc₃ stability on TiO₂ electrodes, analysis of fcc₃ adsorption on TiO₂, and decomposition after prolonged irradiation; NMR analysis of light-driven fumarate reduction in solution and corresponding mechanistic studies; and supplementary (photo)-electrochemistry experiments, including Co–Pi deposition on W–BiVO₄, electrode stabilities, and photoelectrochemistry experiments with inverse connections. This material is available free of charge via the Internet at <http://pubs.acs.org>.

■ AUTHOR INFORMATION

■ Corresponding Author

fraser.armstrong@chem.ox.ac.uk

■ Notes

The authors declare no competing financial interest.

■ ACKNOWLEDGMENTS

This research was supported by BBSRC (Grants BB/I022309-1, BB/L009722/1) and EPSRC (Supergen V Grant EP/H019480/1). A.B. thanks St. John's College Oxford for a Graduate Scholarship. F.A.A. is a Royal Society-Wolfson Research Merit Award holder. We thank Profs. S. K. Chapman and G. Reid for providing initial samples of fcc₃, Prof. J. Durrant for supplying nonscattering TiO₂ particles, and Prof. M. Hayward for providing access to a high-temperature furnace.

■ REFERENCES

- (1) Lewis, N. S.; Nocera, D. G. *Proc. Natl. Acad. Sci. U.S.A.* **2006**, *103*, 15729.
- (2) Jacobsson, T. J.; Fjällström, V.; Sahlberg, M.; Edoff, M.; Edvinsson, T. *Energy Environ. Sci.* **2013**, *6*, 3676.
- (3) Khaselev, O.; Turner, J. A. *Science* **1998**, *280*, 425.

- (4) Reece, S. Y.; Hamel, J. A.; Sung, K.; Jarvi, T. D.; Esswein, A. J.; Pijpers, J. J. H.; Nocera, D. G. *Science* **2011**, *334*, 645.
- (5) Abdi, F. F.; Han, L.; Smets, A. H. M.; Zeman, M.; Dam, B.; van de Krol, R. *Nat. Commun.* **2013**, *4*, 2195.
- (6) Cuendet, P.; Grätzel, M. *Photochem. Photobiol.* **1984**, *39*, 609.
- (7) Kim, Y.; Ikebukuro, K.; Muguruma, H.; Karube, I. *J. Biotechnol.* **1998**, *59*, 213.
- (8) Jiang, Z.; Lü, C.; Wu, H. *Ind. Eng. Chem. Res.* **2005**, *44*, 4165.
- (9) Lu, J.; Li, H.; Cui, D.; Zhang, Y.; Liu, S. *Anal. Chem.* **2014**, *86*, 8003.
- (10) Song, W.; Vannucci, A. K.; Farnum, B. H.; Lapidus, A. M.; Brennaman, M. K.; Kalanyan, B.; Alibabaei, L.; Concepcion, J. J.; Losego, M. D.; Parsons, G. N.; Meyer, T. J. *J. Am. Chem. Soc.* **2014**, *136*, 9773.
- (11) *Molecular to Global Photosynthesis*; Archer, M. D., Barber, J., Eds.; Imperial College Press: London, 2004.
- (12) Taylor, P.; Pealing, S. L.; Reid, G. A.; Chapman, S. K.; Walkinshaw, M. D. *Nat. Struct. Mol. Biol.* **1999**, *6*, 1108.
- (13) Morris, C. J.; Black, A. C.; Pealing, S. L.; Manson, F. D.; Chapman, S. K.; Reid, G. A.; Gibson, D. M.; Ward, F. B. *Biochem. J.* **1994**, *302*, 587.
- (14) Vincent, K. A.; Parkin, A.; Armstrong, F. A. *Chem. Rev.* **2007**, *107*, 4366.
- (15) Hoertz, P. G.; Chen, Z.; Kent, C. A.; Meyer, T. J. *Inorg. Chem.* **2010**, *49*, 8179.
- (16) Kato, M.; Cardona, T.; Rutherford, A. W.; Reisner, E. *J. Am. Chem. Soc.* **2012**, *134*, 8332.
- (17) Bachmeier, A.; Wang, V. C. C.; Woolerton, T. W.; Bell, S.; Fontecilla-Camps, J. C.; Can, M.; Ragsdale, S. W.; Chaudhary, Y. S.; Armstrong, F. A. *J. Am. Chem. Soc.* **2013**, *135*, 15026.
- (18) Hexter, S. V.; Grey, F.; Happe, T.; Climent, V.; Armstrong, F. A. *Proc. Natl. Acad. Sci. U.S.A.* **2012**, *109*, 11516.
- (19) Murphy, B. J.; Sargent, F.; Armstrong, F. A. *Energy Environ. Sci.* **2014**, *7*, 1426.
- (20) Turner, K. L.; Doherty, M. K.; Heering, H. A.; Armstrong, F. A.; Reid, G. A.; Chapman, S. K. *Biochemistry* **1999**, *38*, 3302.
- (21) Walter, M. G.; Warren, E. L.; McKone, J. R.; Boettcher, S. W.; Mi, Q.; Santori, E. A.; Lewis, N. S. *Chem. Rev.* **2010**, *110*, 6446.
- (22) Reisner, E.; Fontecilla-Camps, J. C.; Armstrong, F. A. *Chem. Commun.* **2009**, 550.
- (23) Woolerton, T. W.; Sheard, S.; Reisner, E.; Pierce, E.; Ragsdale, S. W.; Armstrong, F. A. *J. Am. Chem. Soc.* **2010**, *132*, 2132.
- (24) Gross, M. A.; Reynal, A.; Durrant, J. R.; Reisner, E. *J. Am. Chem. Soc.* **2014**, *136*, 356.
- (25) Ye, H.; Park, H. S.; Bard, A. J. *J. Phys. Chem. C* **2011**, *115*, 12464.
- (26) Hong, S. J.; Lee, S.; Jang, J. S.; Lee, J. S. *Energy Environ. Sci.* **2011**, *4*, 1781.
- (27) Kanan, M. W.; Nocera, D. G. *Science* **2008**, *321*, 1072.
- (28) Zhong, D. K.; Cornuz, M.; Sivula, K.; Grätzel, M.; Gamelin, D. R. *Energy Environ. Sci.* **2011**, *4*, 1759.
- (29) The fuel-forming reaction is our reaction of interest; for experiments with inverse connections, i.e., Co–Pi-modified W–BiVO₄ as the WE and fcc₃–ITO as the CE, see the SI.
- (30) Abdi, F. F.; Firet, N.; van de Krol, R. *ChemCatChem* **2013**, *5*, 490.
- (31) Chen, Z.; Dinh, H. N.; Miller, E. *Photoelectrochemical Water Splitting: Standards, Experimental Methods, and Protocols*; Springer: New York, 2013.
- (32) Bornoz, P.; Abdi, F. F.; Tilley, S. D.; Dam, B.; van de Krol, R.; Grätzel, M.; Sivula, K. *J. Phys. Chem. C* **2014**, *118*, 16959.